Observation of High Transformer Ratio of Shaped Bunch Generated by an Emittance-Exchange Beam Line

Q. Gao, G. Ha, C. Jing, S. P. Antipov, J. G. Power, M. Conde, W. Gai, H. Chen, J. Shi, E. E. Wisniewski, D. S. Doran, W. Liu, C. E. Whiteford, A. Zholents, P. Piot, and S. S. Baturin

Phys. Rev. Lett. **120**, 114801 — Published 13 March 2018

DOI: 10.1103/PhysRevLett.120.114801

Observation Of High Transformer Ratio Of Shaped Bunch Generated By Emittance-Exchange Beam Line

Q. Gao,[1,2,*] G. Ha,[3] C. Jing,[4] S. P. Antipov,[4] J. G. Power,[5] M. Conde,[5] W. Gai,[5] H. Chen,[1] J. Shi,[1,†] E. E. Wisniewski,[5] D. S. Doran,[5] W. Liu,[5] C. E. Whiteford,[5] A. Zholents,[5] P. Piot,[6,7] and S. S. Baturin[8]

[1]*Department of Engineering Physics, Tsinghua University Beijing 100084, P.R. China*
[2]*Key Laboratory of Particle and Radiation Imaging (Tsinghua University), Ministry of Education, Beijing 100084, P.R. China*
[3]*POSTECH, Pohang, Gyeongbuk 37673, Republic Of Korea*
[4]*Euclid Techlabs LLC, Bolingbrook, Illinois 60440, USA*
[5]*Argonne National Laboratory, Lemont, Illinois 60439, USA*
[6]*Department of Physics, Northern Illinois University, DeKalb, IL 60115, USA*
[7]*Fermi National Accelerator Laboratory, Batavia, IL 60510, USA.*
[8]*The University of Chicago, PSD, Enrico Fermi Institute, 5640 S Ellis Ave, Chicago, IL 60637, USA*

(Dated: December 22, 2017)

Collinear wakefield acceleration has been long-established as a method capable of generating ultra-high acceleration gradients. Due to the success on this front, recently, more efforts have shifted towards developing methods to raise the transformer ratio (TR). This figure of merit is defined as the ratio of the peak acceleration field behind the drive bunch to the peak deceleration field inside the drive bunch. TR is always less than two for temporally symmetric drive bunch distributions and therefore recent efforts have focused on generating asymmetric distributions to overcome this limitation. In this paper, we report on using the emittance-exchange method to generate a shaped drive bunch to experimentally demonstrate a $TR \approx 5$ in a dielectric wakefield accelerator.

Beam-driven collinear wakefield accelerators (CWA) are promising candidates for next generation linear colliders and compact short-wavelength multiuser free electron laser (FEL) facilities [1–4]. In this scheme, a trailing low-charge witness electron bunch gets accelerated by the wakefield excited by a preceding high-charge drive electron bunch traveling on the same path in a high impedance structure, such as dielectric-loaded waveguide or a medium, such as plasma [5–7]. Two key figures of merit in the CWA scheme are the accelerating gradient (E_z) and the transformer ratio (TR), which both depend on the temporal distribution of the drive bunch [8]. TR is defined as the ratio of peak acceleration field (E_z^+) behind the drive bunch to the peak deceleration field (E_z^-) inside the drive bunch [9]. It determines the maximum energy gain of the witness bunch when the drive bunch loses all of its energy in a CWA linac of length L_l: $\Delta\mathcal{E} = e \cdot L_l \cdot E_z^+ = e \cdot L_l \cdot TR \cdot E_z^-$, where e is the electron charge. If TR is higher, then the required drive bunch energy is lower and the length of the CWA linac needed is shorter to achieve a given witness bunch energy gain. This implies that the construction cost of a CWA facility could be significantly lowered by raising TR.

Since TR is always less than two for temporally symmetric drive bunch distributions and linear media [10, 11], generating asymmetric distributions to overcome this limitation has become an active area of research. The first successful method to overcome this limit used a ramped train of drive bunches with progressively increasing charge to experimentally demonstrate TR of 2.3, subsequently increased to 3.4 [12–14]. However, since TR is proportional to the length of the train, it becomes difficult to increase TR significantly above this level due to the high charge requirement. Other researchers have developed methods for shaping the temporal distribution of a single drive bunch: laser-shaping at the photocathode method [15] and correlation-based methods [16, 17].

In this Letter, we use an emittance-exchange (EEX) beamline to map the initial horizontal distribution into a precise final current profile [18]. Compared to previous methods, the EEX method is capable of generating accurate temporal shapes due to the ease of controlling the transverse phase space distribution before the EEX beamline via a mask [19]. We report on the observation of a high transformer ratio generated by a shaped drive bunch with a quasi-triangular current profile generated by the EEX beamline at the Argonne Wakefield Accelerator (AWA) [20]. In contrast with previous experiments, where TR was indirectly measured or referred, we were able to directly measure TR due to the development of a novel single-shot wakefield mapping method. The results demonstrate that TR higher than 4.5 is achieved.

The experimental setup is shown in Fig. 1. A 20-nC, 8 MeV electron bunch is generated by an L-band 1.5 cell photoinjector and accelerated by 6 standing-wave accelerating structures (not shown) to 48 MeV. The linac phase is negative 15 degree with respect to crest (0°) in order to suppress the energy chirp. This bunch is then sent into the experimental area containing the EEX beamline consisting of the transverse-deflecting cavity (TDC1) flanked by two identical dogleg sections.

Considering an electron with an initial horizontal phase space coordinate (x_i, x_i'), its final longitudinal position at the downstream of the EEX beamline is given by

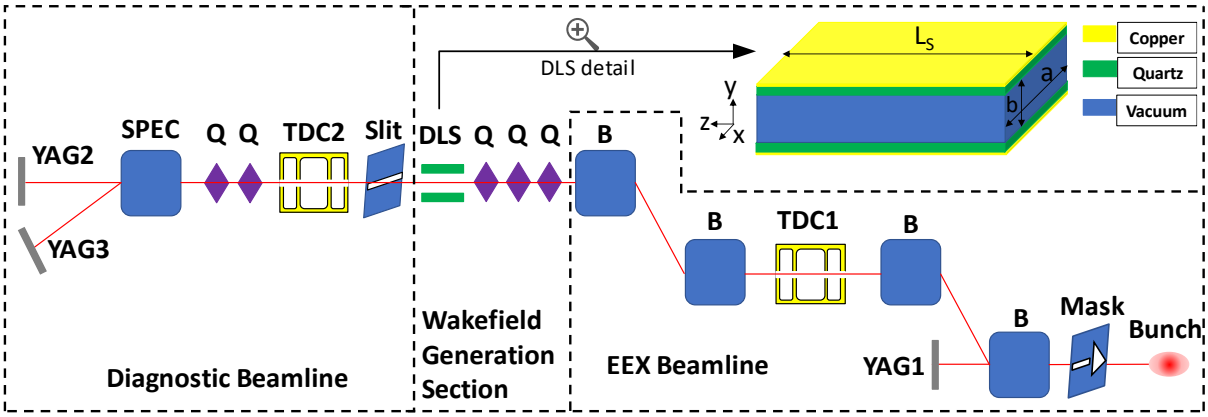

FIG. 1. Schematic of beamline, B, TDC, Q, DLS and SPEC stand for dipole, transverse deflecting cavity, quadrupole, dielectric-loaded structure and spectrometer. YAG represents the beam image observation station.

$z_f = \{\kappa\xi + S_x[\eta + \kappa\xi(L + L_D)]\}x_i$ under the thin-lens and linear dynamics approximation while ignoring collective effects [20]. In the previous equation, all the coordinates are referenced with respect to the bunch barycenter, the parameter $S_x \equiv x_i'/x_i$ refers to linear relationship between x_i' and x_i, κ is the dimensionless TDC strength, ξ and η refer to the momentum compaction factor and dispersion associated with one dogleg, L and L_D represent the R_{12} term of dogleg transport matrix and the drift length between TDC1 and dipole, respectively. Based on this principle, an arbitrary horizontal distribution at entrance of the EEX can be mapped to the longitudinal space at the exit of the EEX with a linear compression factor equal to the term inside the curly braces.

A tungsten mask, which is shown in Fig. 1, is placed at the entrance to the EEX to tailor the drive bunch into a quasi-triangular horizontal shape and the witness bunch into a rectangular horizontal shape whose length is at least twice as the designed fundamental wakefield wavelength. These horizontal distributions are mapped by the EEX into longitudinal ones and sent into a dielectric-loaded structure (DLS) with a variable gap for wakefield excitation and measurement. The DLS geometry is shown in top right corner of Fig. 1, its dielectric liner consists of a 150-μm thickness layer of quartz with a permittivity $\epsilon_r = 3.75$ and copper coating on one side. The total length L_S and width a of the structure is 15 cm and 1.27 cm. The largest achievable gap b (vacuum region between the two layers of quartz) reaches 3.1 cm corresponding to the case where the wakefield is 10,000 times weaker than the gap of 2.5 mm. During our experiment, the gap size was set to 2.5 ± 0.2 mm and 2.1 ± 0.2 mm corresponding to a predicted fundamental wakefield frequency of $121.9^{+4.1}_{-3.7}$ and $130.7^{+5.3}_{-4.7}$ GHz, respectively. Downstream of the DLS, the diagnostic beamline consists of a vertical TDC2 (kicks beam in the y-direction) and a horizontal spectrometer (bends the beam in the x-direction), for measurement of the longitudinal phase space (LPS). This allows for a single-shot wakefield mapping to explicitly measure TR. A slit with a vertical aperture 100 μm is placed between the DLS and TDC2 to improve the resolution of energy measurement [21]. Theoretical analysis indicates that the LPS system has an energy resolution of 30 keV and time resolution is 0.124 ps.

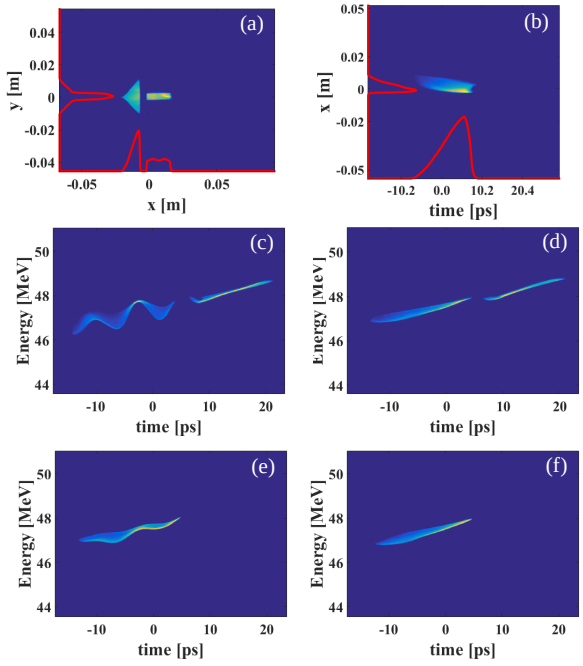

FIG. 2. Beam Image From Experiment: (a) Drive and witness transverse distribution at YAG1, red line refers to projection. (b) Longitudinal profile measurement result of drive bunch at YAG2. (c-d) Drive and witness bunch at YAG3 with wakefield on/off. (e-f) Witness bunch at YAG3 with wakefield on/off.

The experimental results are shown in Figure 2. The horizontal beam distribution observed at YAG1 is shown

in Fig. 2 (a). At this location the beam is tailored transversely by the mask to form a quasi-triangular drive bunch and long rectangular witness bunch [as seen in the projection of Fig. 2 (a)]. Downstream of the EEX beamline, the time-domain distribution of drive bunch is measured by TDC2 as shown in Fig. 2 (b). The sharp tail of the triangle is slightly stretched due to coherent synchrotron radiation (CSR) [22] in the dogleg. The sequences of images in Fig. 2(c-f) were taken at YAG3 located behind the spectrometer with TDC2 on and represent the single-shot measurement of the LPS for different DLS configurations. In (c) and (e), Wakefield-on corresponds to a DLS gap of 2.5 mm, while in (d) and (f), wakefield-off refers to a DLS gap of 31 mm. All the machine parameters were kept identical while taking data except for the DLS gap size. The shaped drive bunch in the wakefield-on case excites a wakefield which modulates the trailing witness bunch energy distribution as seen in Fig. 2(c). In the contrast, in the wakefield-off case, both the drive and witness have their LPS unaltered, see Fig. 2(d). The transmitted charge of the drive bunch after the DLS is $2.08^{+0.15}_{-0.10}$ nC and the witness is $1.06^{+0.10}_{-0.08}$ nC. Fig. 2(e) and Fig. 2(f) indicate that the witness-bunch charge is high enough to induce a self-modulation which is taken into account during the analysis below.

The wakefield generated by the measured drive bunch distribution is calculated from Fig. 2(c-f) in the following steps. First, the LPS envelope is extracted out from the individual images as exemplified in Fig. 3(a), where the witness self-wakefield modulation is subtracted out. Second, the average profile of each LPS envelope is calculated as shown in Fig. 3(b). Since the wakefield measurement is sensitive to the drive charge level as well as its energy jitter, the average profile fluctuation in the LPS is computed over several shots as presented in Fig. 3(c). Finally, the average LPS associated with the wakefield-off case is subtracted from the wakefield-on case to yield the wakefield generated by the shaped drive bunch as exhibited in Fig. 3(d). TR is calculated as the ratio of the maximum witness-bunch energy gain to the maximum drive-bunch energy loss from the measured wakefield data, and the error bar is calculated from the average profile fluctuation shown in Fig. 3(c).

We calculated the analytical wakefield of the DLS with a code using the method published in [23] and the measured current profile. The total field induced in the DLS can be constructed as a sum of eigen-modes, which are commonly categorized as longitudinal section magnetic (LSM_{mn}) modes and longitudinal section electric (LSE_{mn}) modes [24], where m and n refer to index of roots for dispersion equations. For a given gap size, dielectric material, dielectric layer thickness and width, the Green's function associated with each eigen-mode is calculated. Here we use a 1-D longitudinal charge distribution for the drive and witness bunch traveling on the center axis of the DLS. We used 80 x-modes and 10 y-modes of both LSM_{mn} and LSE_{mn} since contributions from the higher order modes are down by a factor of 2,500. The longitudinal wakefield is computed from,

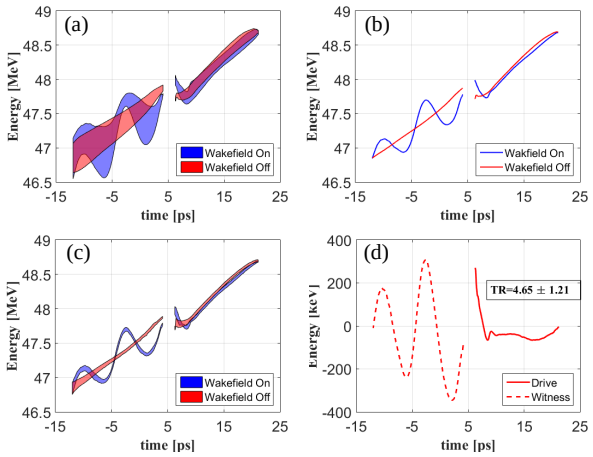

FIG. 3. Reconstructed longitudinal phase space and measured wakefield: (a) Longitudinal phase space full envelope. (b)Average profile in LPS. (c) Average profiles error bar in LPS. (d) Measured energy gain induced by wakefield.

$$W_z(t) = \int_0^t \sum_{m=1}^{80} \sum_{n=1}^{10} I(\tau) G_{mn}(t-\tau) d\tau \qquad (1)$$

where $G_{mn}(t)$ represents the Green's function associated with each eigen-mode and $I(t)$ refers to the drive bunch current profile measured from Fig. 2(b).

The measured wakefield (Fig. 4(a)) is compared to the analytical wakefield (Eq. 1) and used to calulate TR for a DLS gap of 2.5 mm. The measured gradients inside and behind the drive bunch are in good agreement with the analytic predictions including the wakefields in the region near the tail of drive bunch. (The reason the tail of the drive bunch gets accelerated is due to roll-off of the tail.) The value of TR measured from this figure is 4.65 ± 1.21 which is also in good agreement with the analytical value of 4.51. Note that the measured maximum energy gain of the witness bunch is not due to the first acceleration peak since the intercepting mask had a minimum separation of 5 mm and therefore the witness bunch could not sample the first peak. Instead, the witness bunch samples the second acceleration peak of the wakefield where the peak field is 2.05 MV/m. Measuring the wakefields inside the drive bunch is typically challenging [25] but our single-shot LPS measurement method allows us to observe the energy modulation in this region and it agrees well with the analytical one. The measured maximum decelerating gradient inside the drive bunch is 0.44 MV/m. The discrepancy between the measured and analytical value of TR comes primarily from the measurement resolution of the drive bunch energy loss. In the LPS image (Fig. 2), the energy calibration is 9 keV/pixel but the maximum drive bunch energy loss is only approimately 66

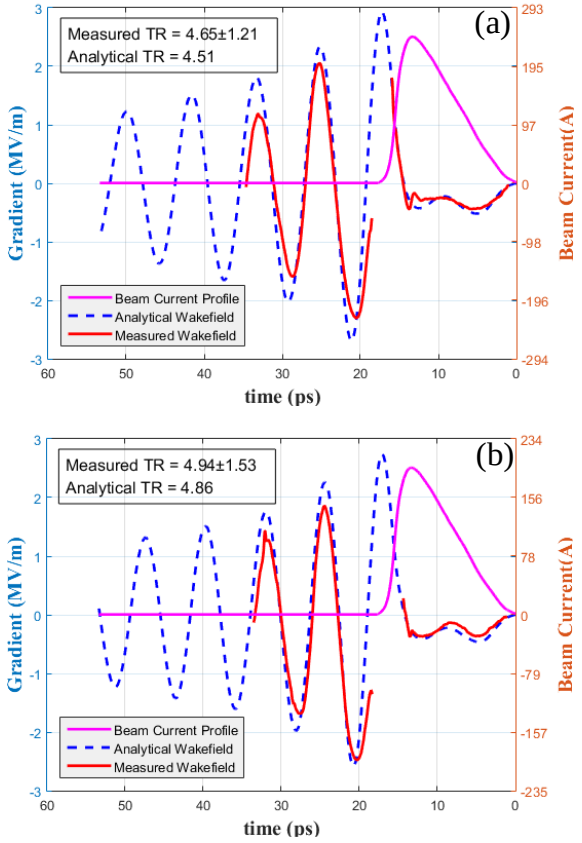

FIG. 4. (a-b) Comparison between measured and analytical wakefield induced by drive bunch when the gap is 2.5 mm (a)/ 2.1 mm (b).

keV, and the data shows that the relative error bar of measured TR is 26%. Finally, the measured wakefield shows the time difference between the two peaks behind drive bunch is 7.9 ps, which is close to the analytical value of 8.1 ps. Therefore, the frequency spectrum of the measured wakefield is close to the analytic one. The decay of the wakefield amplitude seen in Fig. 4(a) is due to dissipation and multi-mode effects.

We note that there is some discrepancy between the measured and analytic wakefield amplitude which we think arises for two reasons. The first reason is that the boundary condition of the DLS in the experiment is an open boundary (adjacent region in the x-direction is vacuum), however, the Green's function is derived from a closed boundary (electric wall) rectangular waveguide model for simplicity since there is no concise analytical solution for an open boundary and the results from numerical simulation tools are limited by the finite mesh. This will act to increase the shunt impedance of the eigenmodes which overestimates the wakefield amplitude in the theoretical model because some of the wakefield energy radiates out from the open boundary during the experiment. The second reason is that the width of the DLS in the x-direction is finite so the Green's function depends on the transverse coordinates. The Green's function we used for the calculation is derived from the central axis $(x = 0, y = 0)$ which is larger than the off-axes position. Since we used strong transverse focusing to transport the beam through the DLS during the experiment, the beam size at the extrance and exit of DLS may be comparable to the structure width there. This means that some of the bunch contributes less energy to the wakefield than on-axis calculation thus causing the measured wakefield amplitude value to be lower than the analytical one.

The measured wakefield (Fig. 4(b)) was also compared to the analytical wakefield (Eq. 1) and used to calulate TR for a DLS gap of 2.1 mm. Since the drive bunch was the same as the 2.5 mm case above, the higher frequency of this DLS structure should yield a higher TR [15]. The transmitted drive charge after the DLS is 1.66 nC in this case. Compared with the larger 2.5 mm gap DLS, the modulation inside drive bunch is more obvious but closely follows the analytic curve. The measured TR of 4.94 ± 1.53 is again in very good agreement with the analytically predicted value of 4.86.

In conclusion, a quasi-triangle shaped bunch is generated using the EEX method and the transformer ratio of this shaped bunch is successfully measured using the single-shot wakefield mapping method. These results demonstrate that TR values in excess of 4.5 are attained which is much higher than the limit of 2 for symmetric current profiles. This result shows the feasibility of a factor of 2 reduction of the linac length or a factor of 2 increase of the achievable witness energy compared to using a drive beam with symmetric longitudinal current distribution in the collinear wakefield accelerator. This is a necessary step to realize a realistic CWA for future high-energy colliders or light sources.

This work is supported by the U.S. Department of Energy, Offices of HEP and BES, under contract No.DE-AC02-06CH11357. It is also funded by the National Natural Science Foundation of China (NSFC) No.11375098.

* gaoq08thu@gmail.com
† shij@mail.tsinghua.edu.cn

[1] B. OShea, G. Andonian, S. Barber, K. Fitzmorris, S. Hakimi, J. Harrison, P. Hoang, M. Hogan, B. Naranjo, O. Williams, *et al.*, Nature communications **7** (2016).
[2] M. Litos, E. Adli, W. An, C. Clarke, C. Clayton, S. Corde, J. Delahaye, R. England, A. Fisher, J. Frederico, *et al.*, Nature **515**, 92 (2014).
[3] C. Jing, S. Antipov, J. Qiu, A. Kanareykin, J. Power, M. Conde, W. Liu, E. Wisniewski, G. Ha, D. Wang, *et al.*, Proc. IPAC **15**, 2714 (2015).
[4] A. Zholents, W. Gai, S. Doran, R. Lindberg, J. Power, N. Strelnikov, Y. Sun, E. Trakhtenberg, I. Vasserman, C. Jing, *et al.*, Nuclear Instruments and Methods in Physics Research Section A: Accelerators, Spectrometers,

Detectors and Associated Equipment **829**, 190 (2016).
[5] W. Gai, P. Schoessow, B. Cole, R. Konecny, J. Norem, J. Rosenzweig, and J. Simpson, Physical review letters **61**, 2756 (1988).
[6] M. Rosing and W. Gai, Physical Review D **42**, 1829 (1990).
[7] P. Chen, J. M. Dawson, R. W. Huff, and T. Katsouleas, Physical Review Letters **54**, 693 (1985).
[8] S. Baturin and A. Zholents, Phys.rev.accel.beams **20** (2017).
[9] K. L. Bane, P. Chen, and P. Wilson, *On collinear wake field acceleration*, SLAC-PUB 3662 (SLAC, 1985).
[10] P.B.Wilson, *Proceedings of 13th SLAC Summer Institute on Particle Physics*, SLAC Report 296 (SLAC, 1973).
[11] J. Power, W. Gai, and P. Schoessow, Physical Review E **60**, 6061 (1999).
[12] C. Jing, A. Kanareykin, J. Power, M. Conde, Z. Yusof, P. Schoessow, and W. Gai, Physical Review Letters **98**, 144801 (2007).
[13] C. Jing, J. Power, M. Conde, W. Liu, Z. Yusof, A. Kanareykin, and W. Gai, Physical Review Special Topics-Accelerators and Beams **14**, 021302 (2011).
[14] G. Sotnikov and T. Marshall, Physical Review Special Topics-Accelerators and Beams **14**, 031302 (2011).
[15] F. Lemery and P. Piot, Physical Review Special Topics-Accelerators and Beams **18**, 081301 (2015).
[16] P. Piot, C. Behrens, C. Gerth, M. Dohlus, F. Lemery, D. Mihalcea, P. Stoltz, and M. Vogt, Physical review letters **108**, 034801 (2012).
[17] R. England, J. Frederico, M. Hogan, C. Joshi, W. An, W. Lu, W. Mori, W. An, P. Muggli, *et al.*, in *Conf. Proc. C110328: 265-267, 2011*, SLAC-PUB-16683 (SLAC National Accelerator Laboratory (SLAC), 2016).
[18] B. Jiang, C. Jing, P. Schoessow, J. Power, and W. Gai, Physical Review Special Topics-Accelerators and Beams **15**, 011301 (2012).
[19] P. Piot, Y.-E. Sun, J. Power, and M. Rihaoui, Physical Review Special Topics-Accelerators and Beams **14**, 022801 (2011).
[20] G. Ha, M. Cho, W. Namkung, J. Power, D. Doran, E. Wisniewski, M. Conde, W. Gai, W. Liu, C. Whiteford, *et al.*, Physical Review Letters **118**, 104801 (2017).
[21] M. Rihaoui, D. Mihalcea, W. Gai, P. Piot, and J. Power, in *AIP Conference Proceedings*, Vol. 1299 (AIP, 2010) pp. 570–574.
[22] G. Ha, M. Cho, W. Gai, K.-J. Kim, W. Namkung, and J. Power, Physical Review Accelerators and Beams **19**, 121301 (2016).
[23] S. Baturin, I. Sheinman, A. Altmark, and A. Kanareykin, Physical Review Special Topics-Accelerators and Beams **16**, 051302 (2013).
[24] K. Zhang and D. Li, *Electromagnetic theory for microwaves and optoelectronics* (Springer Science & Business Media, 2013).
[25] H. Figueroa, W. Gai, R. Konecny, J. Norem, A. Ruggiero, P. Schoessow, and J. Simpson, Physical review letters **60**, 2144 (1988).